

# **Towards Fail-Safe and Optimized Lightweight Gears: Experimental Analysis of Fatigue Performance and Crack Propagation**

**Author:** Andrea Mura<sup>a</sup>

<sup>a</sup> Politecnico di Torino Department of Mechanical and Aerospace Engineering – C.so Duca degli Abruzzi 24, 10129 Torino Italy.

**Corresponding Author:** Andrea Mura, Politecnico di Torino Department of Mechanical and Aerospace Engineering – C.so Duca degli Abruzzi 24, 10129 Torino Italy.

Tel. ++39 011 090 5907, Fax: ++39 011 090 6999, e-mail [andrea.mura@polito.it](mailto:andrea.mura@polito.it)

## **Abstract**

The structural integrity of gears is crucial for their performance and longevity, particularly in applications where safety is crucial, as in aeronautical applications. In particular, thin-rim gears may face catastrophic or safe failure according to the crack propagation direction. Experimental data about this topic are very rare in the literature. This study investigates the effects of gear geometry, specifically the backup ratio, on crack propagation behavior and fatigue limit by means of experimental fatigue tests performed using an original setup of single-tooth bending test. Results confirmed that gears with lower backup ratios exhibit higher stress concentrations and an increased likelihood of catastrophic failure. Comparisons with existing literature suggest that for intermediate backup ratios, crack propagation direction is influenced by both geometry and operational factors such as centrifugal loads. The findings provide essential insights into gear design optimization, emphasizing the importance of backup ratio selection in ensuring safe and predictable failure modes.

**Keywords:** lightweight gears, fatigue, crack propagation, testing, failsafe design, optimization

## 1. Introduction

In applications where weight reduction is crucial, minimizing the amount of material used in all system components becomes essential. Gears, being critical load-transmitting elements, can also be optimized for weight by removing material in the area between the base of the teeth and the hub. This design approach leads to the development of so-called lightweight or thin-rim gears.

However, while reducing mass, this geometry introduces significant challenges in terms of structural reliability. In particular, it becomes critical to account for failure mechanisms associated with crack propagation. A crack initiating at the tooth root can propagate either radially through the rim, leading to catastrophic failure with the loss of a large portion of the gear, or across the tooth thickness, resulting in the loss of a single tooth and representing a fail-safe condition [1].

Linear elastic fracture mechanics establishes that cracks propagate unstably to rupture when the stress intensity factor reaches the critical threshold  $K_{Ic}$ . It is assumed that the crack advances in the direction corresponding to the maximum mode I stress intensity factor,  $K_I$  [2]. Furthermore, the area where the maximum tensile stress occurs, typically at the tooth root, is considered the primary site for crack nucleation. As the crack grows, the propagation angle decreases, and the path follows the stress field influenced by the geometry and loading conditions [2].

The position along the tooth root where cracks are most likely to nucleate is characterized by the angle  $\varphi$ , defined as the angle between the tooth's line of symmetry and the tangent

to the fillet. It has been observed that the most stressed point typically occurs at  $\phi = 30^\circ$ – $34^\circ$  [3].

Tooth or rim failure depends primarily on the backup ratio  $m_b$ , defined as the ratio of rim thickness to tooth height, and on operational conditions such as misalignment or excessive loading. For  $m_b$  values less than 1.2, cracks tend to propagate radially through the rim, leading to rim fractures [4].

Lewicki et al. [5] conducted a numerical study to investigate how crack propagation behavior changes with varying rim thicknesses. Their analysis covered several gears with different backup ratios and showed that, for all cases,  $K_I$  was consistently larger than  $K_{II}$ . For  $m_b = 0.5$ ,  $K_{II}$  approached zero, leading to cracks propagating in a straight line. For  $m_b > 0.5$ ,  $K_{II}$  became negative, implying a positive propagation angle and resulting in cracks confined within the tooth width, eventually causing tooth detachment. In contrast, for  $m_b < 0.5$ ,  $K_{II}$  was positive, and the crack propagated radially through the rim [5].

It is well established that while  $K_I$  governs the crack propagation rate,  $K_{II}$  influences the deviation of the propagation path. Specifically, if  $K_{II}$  equals zero, cracks propagate straight [6].

Initial crack orientation also significantly affects propagation. For instance, in gears with  $m_b = 3.3$ , cracks consistently propagate along the tooth width, regardless of initial orientation. For  $m_b = 0.2$ , cracks invariably propagate radially, while for  $m_b = 0.5$ , behavior is unstable: horizontal cracks propagate through the tooth, but inclined cracks promote rim fracture [5].

These results closely match experimental observations, except in the critical case of  $m_b = 0.5$ , where multiple outcomes are possible. Moreover, centrifugal forces further influence crack propagation: high rotational speeds increase the likelihood of rim fractures, while low

speeds favor tooth breakage. This behavior stems from the fact that centrifugal loads alter the stress field, thereby modifying the crack propagation angle, which depends on the  $K_{II} / K_I$  ratio [6].

The initial crack nucleation site significantly affects the subsequent propagation path [7]. Generally, higher  $\phi$  angles at the tooth root increase the tendency for cracks to grow along the tooth width. The fillet shape also influences crack behavior: an oversized fillet reduces local stresses and slightly favors tooth failure over rim failure [7].

Similarly, the pressure angle impacts crack propagation: gears with higher pressure angles, characterized by wider bases and sharper heads, exhibit a greater tendency for cracks to propagate along the tooth width rather than radially through the rim [7].

Kramberger et al. [8] investigated crack behavior in various lightweight gear geometries. They examined three configurations: a no-web (tube gear), a web placed at the mid-face width, and a web placed on one side. Their results demonstrated that the no-web design exhibited the longest fatigue life due to the lowest stress intensity factors. In contrast, configurations with non-centrally located webs promoted faster crack growth, with the asymmetric web placement showing the worst performance.

This phenomenon is attributed to the fact that as rim thickness decreases, cyclic compressive stresses near the fillet increase, slowing crack growth and extending fatigue life [9]. Consequently, the design and positioning of internal webs become critical for optimizing durability in thin-rim gears.

Surface finish also plays a vital role in fatigue performance. In the absence of surface treatments, cracks typically nucleate at surface defects; therefore, the quality of surface finishing must be carefully controlled to achieve the desired fatigue limits. Surface treatments such as shot peening and carburizing are widely employed to shift crack

nucleation from surface to subsurface, enhancing fatigue strength through residual compressive stresses [9,10].

In unnotched specimens, cracks nucleate at microstructural discontinuities such as inclusions or secondary phases [9]. In standard gears, assuming no additional flank damage, cracks initiate at the tooth root where stress concentrations are maximum [11]. In such cases,  $K_I$  increases almost linearly with crack length, while  $K_{II}$  peaks near the neutral axis and then decreases as the number of teeth increases [11].

It is also important to note that maximum tensile stresses occur on the active flank of the tooth, while compressive stresses dominate on the passive side [12]. Under cyclic loading, these regions become critical sites for crack initiation.

Furthermore, the highest stress concentration during gear meshing occurs when the load is transmitted through the highest point of single tooth contact (HPSTC) [13,14].

Understanding the crack propagation path is particularly crucial for high-reliability applications such as aerospace, where gear failure must be predictable and manageable.

Although a significant body of research exists on the general fatigue behavior of gears [15–25], experimental studies specifically addressing crack propagation paths in thin-rim gears are remarkably rare.

Kramberger et al. [15] focus on the bending fatigue life analysis of thin-rim spur gears employed in truck gearboxes. The study integrates finite element methods (FEM) with linear-elastic fracture mechanics to predict crack initiation and propagation. Fatigue life is divided into two stages: micro-crack initiation and crack growth, underscoring the importance of continuum mechanics-based modeling for enhanced predictive accuracy. Patil et al. [16] conducted experimental investigations on helical gears using a Gear Dynamic Stress Test Rig (GDSTR) equipped with strain gauges and carbon slip rings.

Contact stress was measured under real operating conditions and compared with results from finite element analysis (FEA). The findings demonstrated a strong correlation between experimental and simulated data, validating the experimental setup for contact stress analysis.

Brandão et al. [17] developed a numerical model to predict micropitting and mild wear in spur gears. Dang Van's multi-axial fatigue criterion was applied to assess fatigue crack initiation under mixed-film lubrication conditions. The results emphasized the critical role of surface pressure distributions in predicting surface damage.

Hong et al. [18] proposed a rotating gear test methodology for evaluating bending fatigue under reversed and released loading conditions. Diagnostic tools were employed to determine test termination, providing a reliable experimental framework for the fatigue analysis of gears under high-cycle loading.

Rajesh et al. [19] utilized experimental methods to validate numerical models predicting contact fatigue life (CFL) and bending fatigue life (BFL) in asymmetric helical gears. Their results highlighted the superior CFL performance of asymmetric designs compared to symmetric counterparts.

Argoud et al. [20] investigated the fatigue behavior of case-hardened steel gears through single-tooth bending fatigue (STBF) tests and stress gradient analysis. The observed bimodal fatigue behavior was attributed to differing crack initiation mechanisms. Weres et al. [21] examined the fatigue life of cylindrical gears using a hydraulic testing machine, establishing fatigue life curves and analyzing failure mechanisms under skewed and straight gear configurations.

Gorla et al. [22] assessed the bending and contact fatigue performance of novel steel alloys intended for large gears. Single-tooth fatigue tests and disc-on-disc contact fatigue

tests revealed that innovative bainitic steels exhibit superior fatigue performance and reduced manufacturing distortions relative to traditional materials.

Osakue and Anetor [23] developed a simplified contact stress model for helical gears, incorporating parameters such as helix angles. Experimental validation demonstrated the model's applicability for preliminary fatigue design purposes.

Concli et al. [24] and Bonaiti et al. [25] proposed a multiaxial approach to correlate single-tooth bending fatigue test results with actual meshing gear behavior. This method provided improved predictions of bending fatigue life under realistic operating conditions. Surface treatments can be applied on gears to improve life performance [26-27].

Among the limited available works, Lewicki et al. [7] provided foundational experimental data on crack trajectories. However, their study was limited to spoked gear geometries with artificially introduced notches, which predefined crack initiation points and therefore may not accurately reflect crack behavior in more typical gear designs.

The present study addresses this significant gap by providing new experimental evidence on crack propagation paths in webbed thin-rim gears.

Unlike previous works [1], [7], [28], the current experiments were performed on unnotched teeth, allowing cracks to nucleate naturally under realistic loading conditions. A modified single-tooth bending test methodology was employed to apply cyclic loads and study crack evolution as a function of backup ratio. This modified test allows the application of loading conditions close to the real ones.

By correlating the experimental results with established theoretical models, and finite element simulations [29-32], this work offers a more comprehensive understanding of failure mechanisms in thin-rim gears.

Ultimately, these findings aim to support the development of more reliable lightweight gear designs, enhancing structural safety and fatigue life in critical engineering sectors such as aerospace, automotive, and robotics.

## 2. Methodology

The geometry of thin-rim gears is characterized by two key parameters (see Figure 1): the backup ratio ( $m_b$ ), which is the ratio of the tooth height to the rim thickness ( $H_B$ ), and the web ratio ( $m_w$ ), defined as the ratio of the web thickness ( $W$ ) to the face width ( $L$ ) [14]. A "full gear" refers to a gear where the web thickness equals the face width ( $m_w = 1$ ).

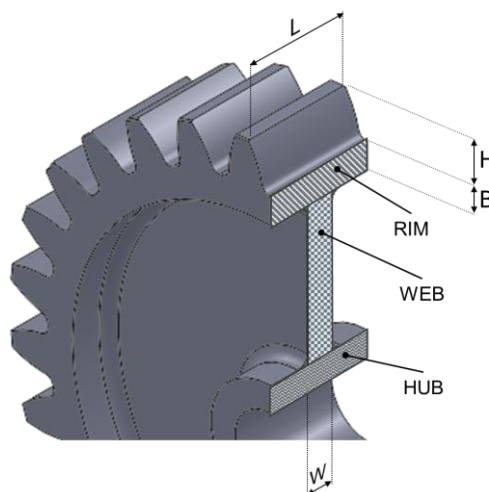


**Figure 1: lightweight gear geometry.**

In this work, three gears made of C55 (without surface or heat treatments) steel have been tested. The three gears have the same tooth geometry (module = 3mm, number of teeth = 32, pressure angle = 20°, no profile shift, face width = 20mm), the only difference lies in the rim thickness, in order to obtain three values of backup ratio (Figure 2).

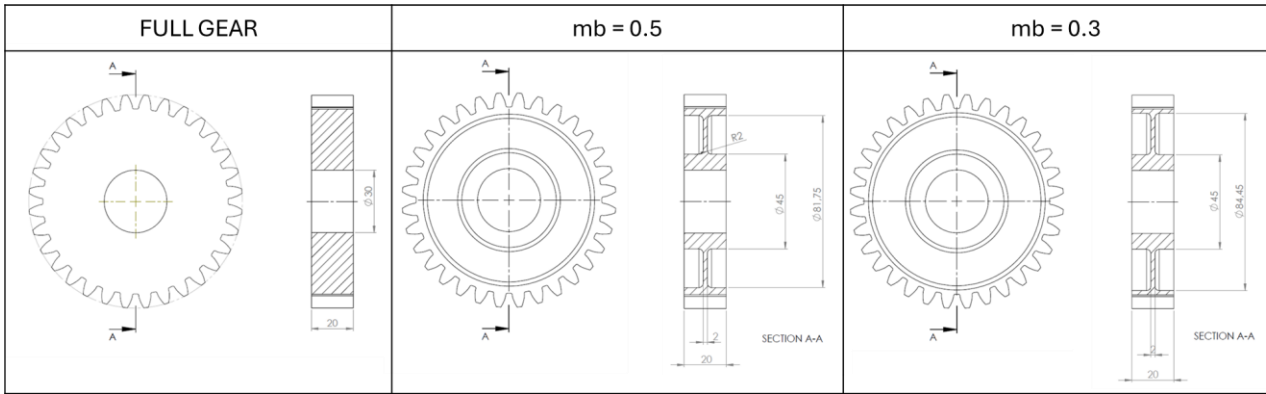


**Figure 2: tested gears geometries.**

The experimental campaign was conducted using a modified single-tooth bending test (STBT), in which the gear hub was rigidly clamped and a cyclic load was applied to a single tooth via a punch (Figures 3 and 4). All tests were performed using an Amsler resonant fatigue testing machine.

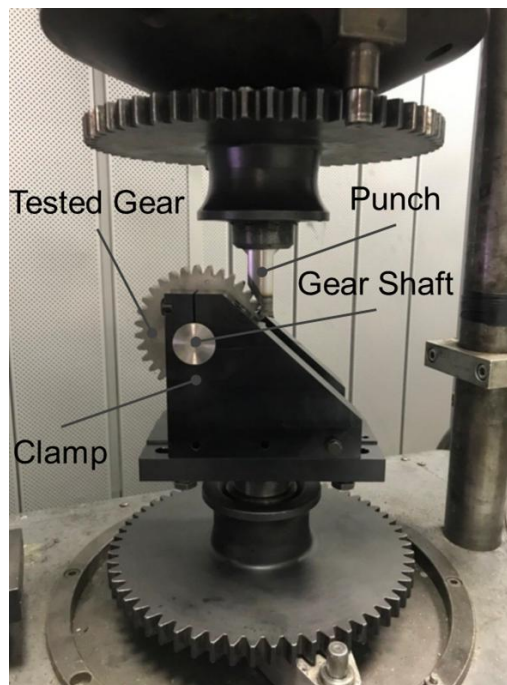


**Figure 3: Single tooth banding test**

The STBT employed in this study differs from the standard configuration, which typically involves loading two teeth [28], as it more accurately replicates the stress distribution from the loaded tooth to the shaft (Figure 4). This setup results in a stress field that more closely resembles actual operating conditions, including in the web region of the gear. Accurately reproducing this stress state is essential for the objectives of this work, which focus on investigating crack propagation paths to prevent catastrophic failures.

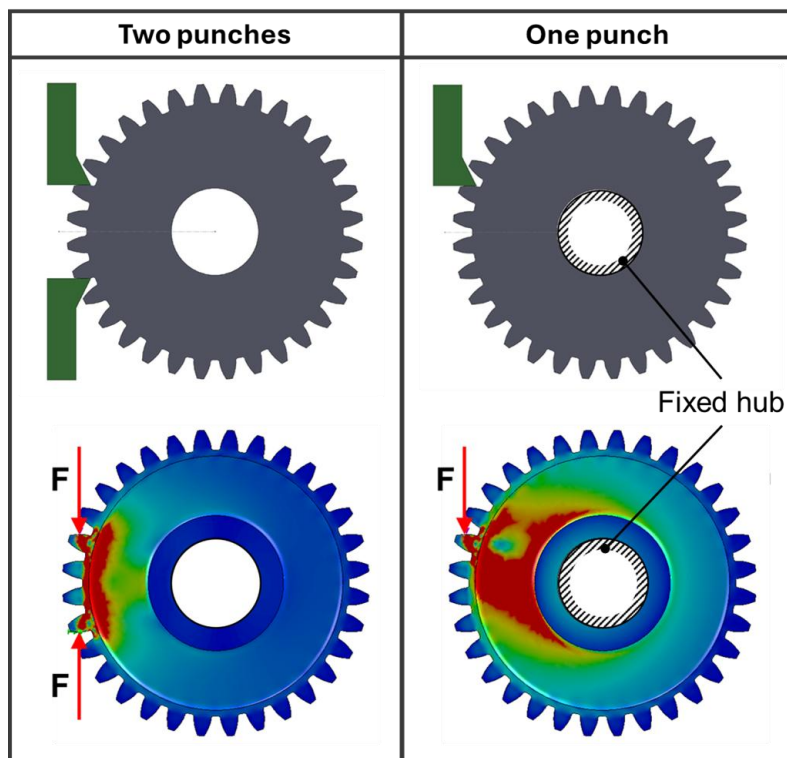


Figure 4: Stress field comparison between two punches (left) and single (right) punch tests.

The fatigue limit of each gear has been obtained according to the Dixon method [33], performing six test on each gear. To avoid the possible influence of broken teeth on the one being tested, each test was conducted on every third tooth (i.e., one tooth was tested, and the next was left untested) [35].

### 3. Results and discussion

### 3.1 Stress analysis

The geometry of the gears can influence both the stress distribution and its magnitude. In this study, the stress distribution of the three investigated gears was analyzed using finite element (FE) models. The primary objective of these models was to determine the location and magnitude of the most highly stressed point.

The FE models were developed using tetrahedral elements, with a refined mesh in the tooth root zone to enhance accuracy, and a coarser mesh in regions where detailed stress analysis was not required. A load was applied along a line across the face width, positioned identically to the experimental setup. The load value was kept constant for all three gears ( $F = 5000 \text{ N}$ ). The gear hub was fixed to define appropriate boundary conditions.

Figure 5 shows the FE results obtained for the three gears.

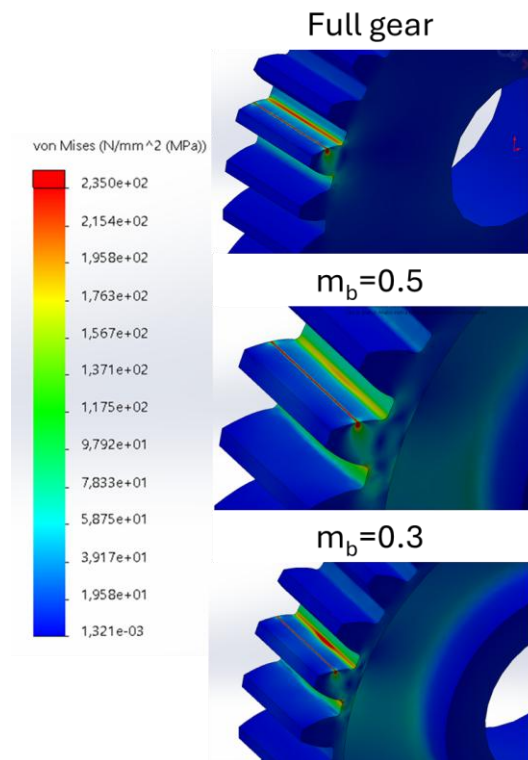


**Figure 5: comparison of the stress distribution in the three gears**

Regarding crack propagation, it is commonly assumed that the crack initiation point corresponds to the point where the maximum stress is reached [10-12], furthermore the crack propagation direction appears to be influenced by the crack initiation position [26-30].

Figure 6 summarizes the location and magnitude of the most stressed point for the three gears. Notably, as the rim thickness decreases (lower value of backup ratio), the most stressed point moves to a position closer to the tooth root [26]. Since cracks are more likely to propagate through the rim when the initiation point is closer to the tooth root, it can be concluded that the crack in the gear with  $m_b=0.3$  is more likely to propagate through the rim compared to the full gear [27-30]. This hypothesis is further supported by the experimental results presented in the next section.

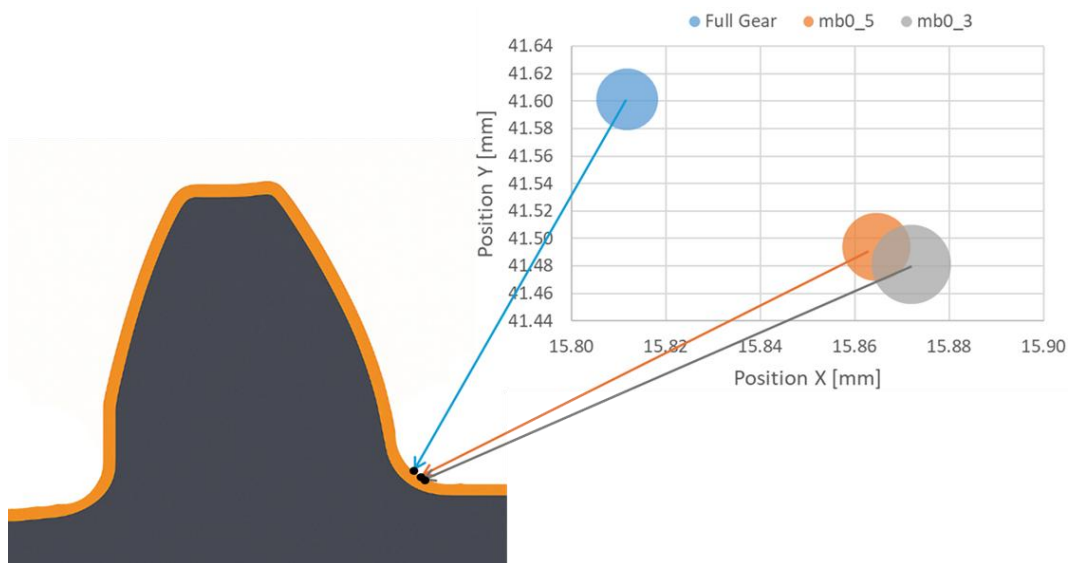


**Figure 6: comparison between stress distributions in the three gears**

The stress magnitude also appears to be influenced by the rim thickness. The results indicate that, for the same applied force, the stress increases as the backup ratio decreases.

### 3.2 Fatigue limits

The fatigue limits of the gears were experimentally determined for the three gears using the Dixon method [33].

Table 1 summarizes the experimental results in terms of fatigue limits considering 50% of non-failure probability ( $\sigma_{F50\%}$ ). The standard deviation of the results indicates that the values obtained for the three gears are comparable.

**Table 1: comparison of fatigue limits obtained by experiments and estimated according is ISO6336 standard [35]**

	<b>Full Gear</b>	<b><math>m_b=0.5</math></b>	<b><math>m_b=0.3</math></b>
<b><math>\sigma_{F50\%}</math> [MPa]</b>	195.2	204.8	182.4
<b><math>\sigma_{Flim}</math> (ISO6336-5) [MPa]</b>	187.9		

The experimental values were compared with the fatigue limit estimated according to the ISO 6336-5 standard [35] ( $\sigma_{Flim}$ ), considering a material hardness of HBW=190.

It should be noted that ISO 6336 standard does not provide design parameters for gears with  $m_b$  lower than 0.5, This limitation is likely due to the fact that in case of lower  $m_b$  values crack propagation may not occur in a safe manner.

### 3.3 Crack propagation analysis

Crack propagation analysis was conducted on broken teeth from the tested gears. For each gear three fractured teeth have been considered.

Figure 7 summarizes crack propagation paths for the three tested gears. The results show that for full gear and gear with  $m_b=0.5$ , cracks propagated through the tooth (safe failure), while in the gear with  $m_b=0.3$ , crack propagation occurred through the rim (catastrophic failure).

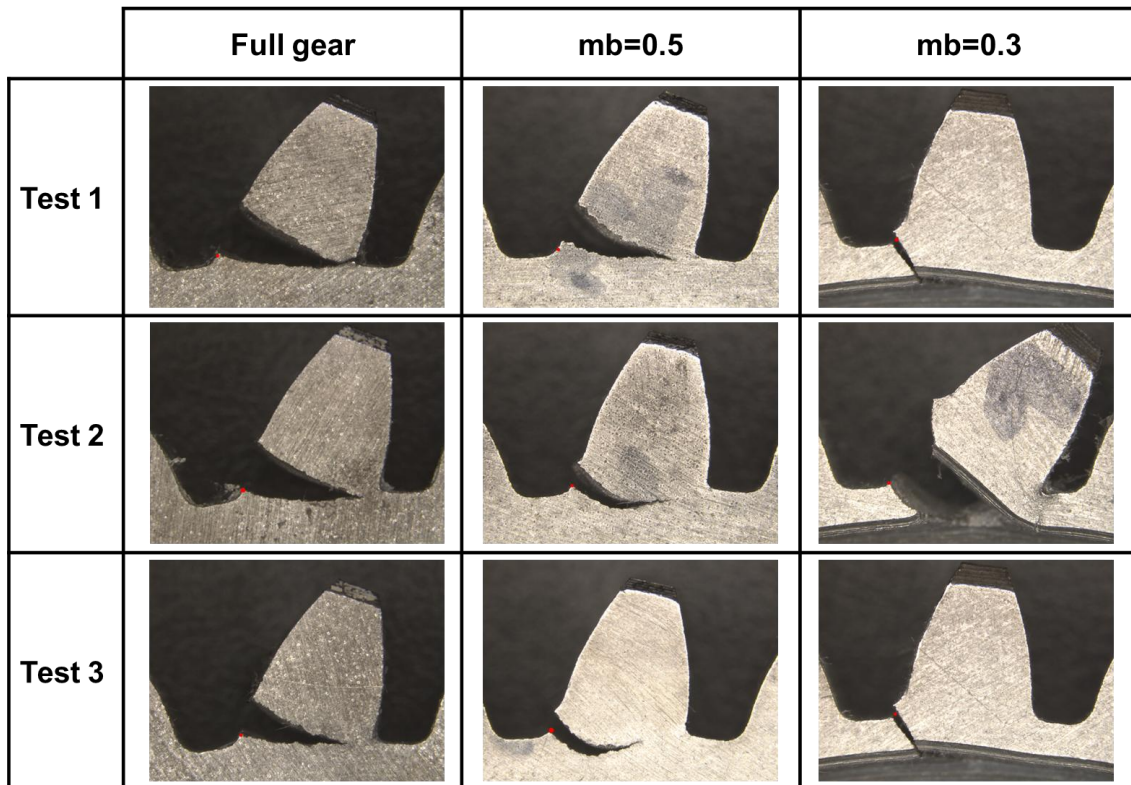


Figure 7: crack paths for the three tested gears and location maximum stressed point found by FE models (red dots).

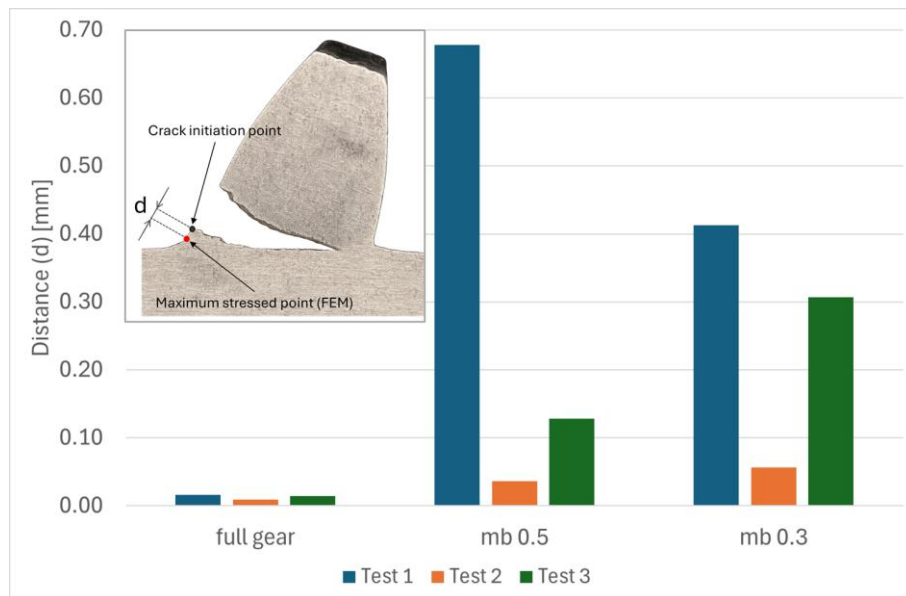
These results are consistent with findings reported in the literature from both numerical and experimental point of view [1], [5-7], [26-32]

In particular, it is interesting to compare the experimental results obtained in this work, with those reported by Lewiki et al [1], [5-7], [30], because the testing procedures used in those studies differ significantly and also the samples geometries is slightly different.

In Figure 7 the small red dots indicate the locations of maximum stress identified through FEM simulations and compare them with the crack initiation points observed in

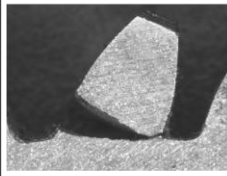
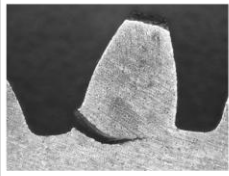
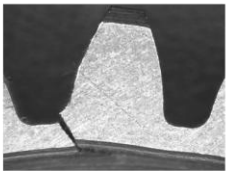
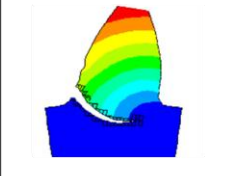
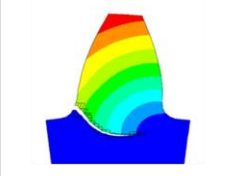
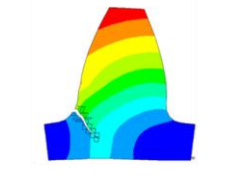
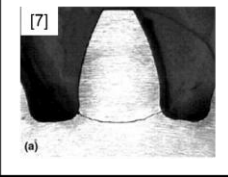
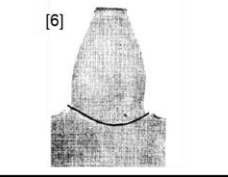
experimental results. The comparison reveals that the crack initiation points align with the maximum stress locations. However, in Test 1 with  $m_b=0.5$ , there is a slight displacement of the crack initiation point.

Figure 8 quantitatively shows the distance between crack initiation points obtained from the experiments and the maximum stressed point obtained by FEM analysis.



**Figure 8: distance between maximum stressed point (obtained by FEM analysis) and crack initiation position.**

Figure 9 presents a comparison between the results obtained in this study and the most relevant findings reported in the literature, including FEM simulations [32] and experimental tests performed on running gears [6–7].

	Full gear ( $m_b=3.3$ )	$m_b=0.5$	$m_b=0.3$
<b>This work</b>			
<b>FEM [32]</b>			
<b>Others experiments [6],[7]</b>			NA

**Figure 9: comparison between results obtained in this work and FEM [32] and running gears [6], [7].**

The comparison highlights that the results obtained in this study are consistent with those reported in the literature. In particular, the crack propagation direction occurs through the tooth in the full gear and through the rim in the gear with  $m_b=0.3$ . Regarding the gear with  $m_b=0.5$ , more detailed considerations are required, as in this case the crack propagation direction depends not only on the gear geometry. This aspect is discussed in the following paragraph.

### 3.3.1 Considerations about the effect of speed

The testing method employed by Lewicki et al. consists of running gears with notched samples, which allows for the reproduction of more realistic operating conditions, as the gears are rotating and the effect of centrifugal load is therefore considered.

On the other hand, the use of notched samples imposes a constraint on the crack initiation location, which could be critical, as for certain values of the backup ratio, the initiation point may influence the crack propagation direction [6], [28], [29], [31] (Figure 10a).

The tests performed in this study were conducted using a single-tooth bending test. In this configuration, the gear is fixed, so the effect of rotational speed is not taken into account. However, due to the high load application frequency (approximately 100 Hz), it was possible to test unnotched gears. As a result, cracks nucleated at “natural” initiation points.

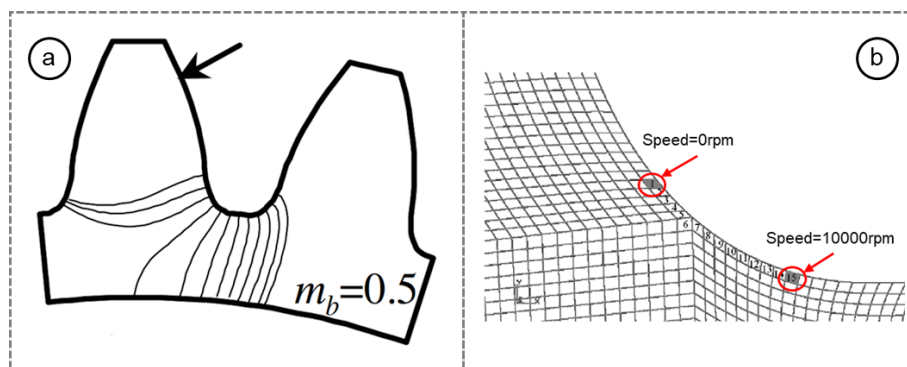


Figure 10: (a) Effect of initial crack location on crack propagation path for a gear with  $m_b=0.5$  [7]; (b) position of maximum stressed point with increasing of speed from 0rpm to 10000rpm [29].

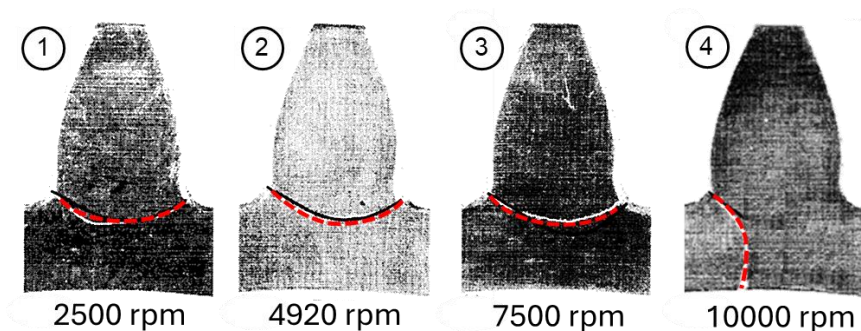


Figure 11: Crack paths with increasing rotating speed for a gear with  $m_b=0.5$  [6]

It is interesting to observe that for backup ratio where the crack propagates always through the tooth ( $m_b > 1$ ) and through the rim ( $m_b < 0.5$ ) the results obtained in this work are consistent with those found in the literature (as shown in Figure 9). For  $m_b = 0.5$  (a value that lies within the range of indeterminacy) the crack propagation direction obtained in this work, is thought the tooth, while in tests with rotating gears the crack propagation direction at this backup ratio, depends on the rotating speed [6], [33] (Figure 11).

In the range of  $m_b$  values associated with indeterminacy, the crack propagation direction is not only affected by the gear geometry (backup ratio), but also by other factors such as the centrifugal load [6], [28], [29]. In particular, the centrifugal load causes the maximum stress point (that is the point where the crack is assumed to initiate) to shift closer to the tooth root (Figure 10b [29]). Consequently, if the crack nucleates closer to the tooth root it is more likely to propagate through the rim (Figure 10a [7]).

### 3.4 Crack surfaces analysis

Crack surfaces were analyzed by SEM on removed teeth from each gear. Figures 12-14 show SEM images and magnifications of one fractured tooth for each gear (respectively the full gear in Figure 12, gear with  $m_b = 0.5$  in Figure 13 and gear with  $m_b = 0.3$  in Figure 14).

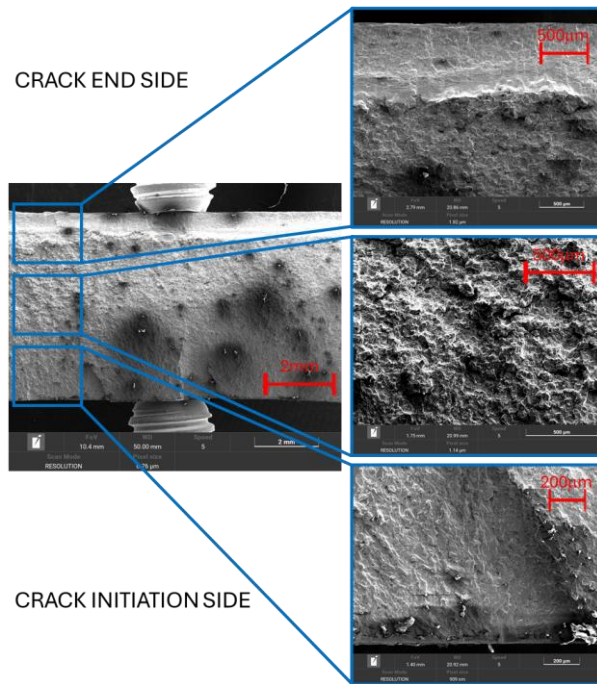


**Figure 12: crack surface for full gear**

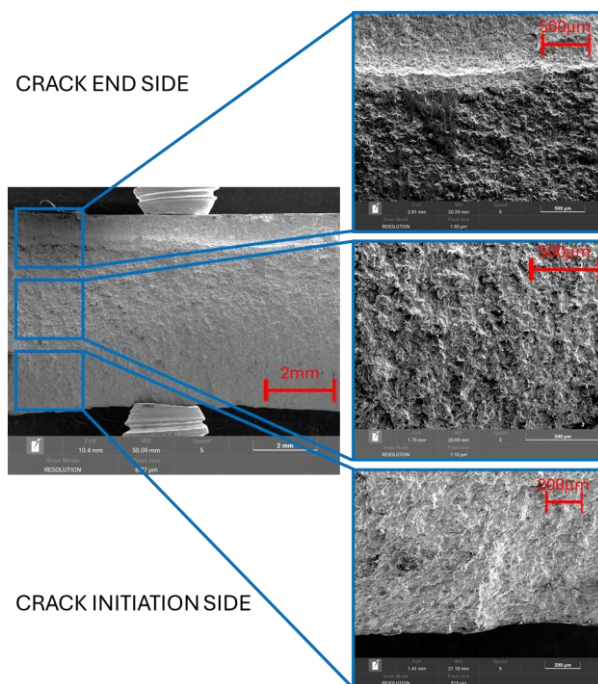


**Figure 13: crack surface for mb =0.5 gear**

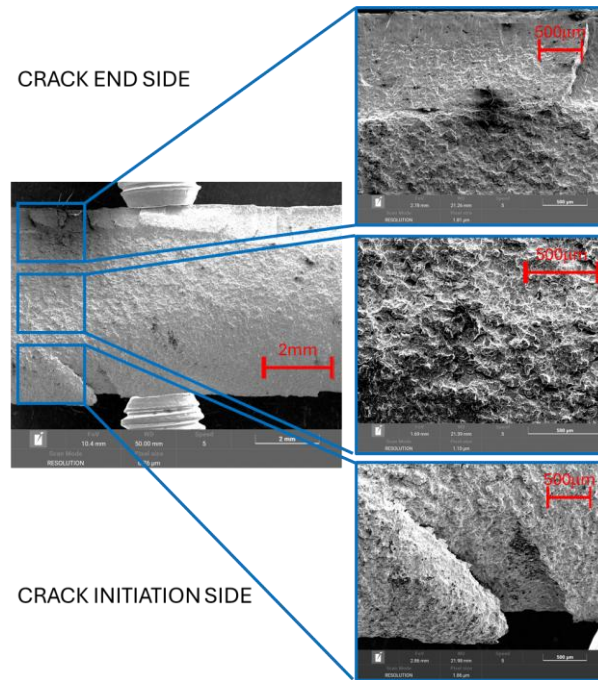


**Figure 14: crack surface for mb =0.3 gear**

In the figures, the crack initiation and arrest sides are shown. It can be observed that, in all analyzed gears, the crack propagation surfaces are not smooth. This is due to the applied load having a mean value slightly higher than the alternating component, which prevents the crack from fully closing during the loading cycle. In contrast, when the mean load is zero, the crack surfaces close during each cycle, producing a hammering effect that smooths the fracture surfaces.

#### **4. Conclusions**

This study investigated crack propagation, fatigue limits, and failure behavior in three different gear gear configurations characterized by varying backup ratios, using a novel experimental approach. Finite element analysis revealed that reducing the rim thickness leads to increased stress magnitudes and shifts the location of the maximum stress closer to the tooth root, significantly affecting crack initiation and propagation behavior.

Experimental fatigue limit tests confirmed that gears with lower backup ratios exhibit higher stress concentrations and a greater likelihood of catastrophic failure. Crack propagation analysis demonstrated that, while gears with higher backup ratios tend to fail safely through the tooth, those with lower ratios ( $m_b = 0.3$ ) exhibit rim propagation, leading to critical failure. These findings are consistent with existing literature and highlight the complex interaction between geometry, stress distribution, and failure modes.

Additionally, comparison with the results of Lewicki et al. suggests that, within the indeterminate range ( $m_b = 0.5$ ), crack propagation direction is influenced not only by gear geometry but also by operational factors such as centrifugal loads. SEM analysis further confirmed that crack surfaces remain rough due to uninterrupted loading, which prevents crack closure and the typical surface smoothing associated with zero-mean load conditions.

Overall, this research provides valuable insights for optimizing gear design, particularly in applications requiring high fatigue resistance and predictable failure mechanisms.

## References

- [1] Lewicki, David G, and Roberto Ballarini. Rim Thickness Effects on Gear Crack Propagation Life, *International journal of Fracture* 87, 1997, pp. 59–86
- [2] Filippini, Mauro, Marco Giglio, Carlo Gorla, and Francesco Rosa., An Integrated Approach for the Prediction of Fatigue Crack Paths in Face Gears for Aerospace Transmissions, *Proceedings of the International Conference on Fatigue Crack Paths (FCP 2003)*, 18-20 September 2003, Parma -Italy.
- [3] Glodez S., Sraml M., Kramberger J., A Computational Model for Determination of Service Life of Gears. *International Journal of Fatigue* 24, fasc. 10 (October 2002): pp. 1013–20. [https://doi.org/10.1016/S0142-1123\(02\)00024-5](https://doi.org/10.1016/S0142-1123(02)00024-5).

- [4] Pandya, Yogesh, and Anand Parey. Crack behavior in a high contact ratio spur gear tooth and its effect on mesh stiffness. *Engineering Failure Analysis* 34 (December 2013): pp. 69–78. <https://doi.org/10.1016/j.engfailanal.2013.07.008>.
- [5] Lewicki, David G. Crack Propagation Studies to Determine Benign or Catastrophic Failure Modes for Aerospace Thin-Rim Gears, NASA Technical Memorandum 107170, May 1996
- [6] Lewicki, G, and U S Army. Effect of Speed (Centrifugal Load) on Gear Crack Propagation Direction, NASA/TM 211117, August 2001
- [7] Lewicki, David G. Gear Crack Propagation Path Studies-Guidelines for Ultra-Safe Design. *Journal of the American Helicopter Society* 47, fasc. 1 (January 1, 2002): pp. 64–72. <https://doi.org/10.4050/JAHS.47.64>.
- [8] Kramberger, J, and J Flašker. Numerical Simulation of 3-D Crack Growth in Thin-Rim Gears, University of Maribor, Proceedings of DESIGN 2002, the 7th International Design Conference, Dubrovnik, 2002, ISBN: 953-6313-45-6.
- [9] Prasannavenkatesan, Rajesh, Jixi Zhang, David L. McDowell, Gregory B. Olson, and Heng-Jeng Jou. 3D Modeling of Subsurface Fatigue Crack Nucleation Potency of Primary Inclusions in Heat Treated and Shot Peened Martensitic Gear Steels. *International Journal of Fatigue* 31, fasc. 7 (July 2009): 1176–89. <https://doi.org/10.1016/j.ijfatigue.2008.12.001>.
- [10] Kramberger, J., M. Šraml, S. Glodež, J. Flašker, and I. Potrč. Computational Model for the Analysis of Bending Fatigue in Gears. *Computers & Structures* 82, fasc. 23–26 (September 2004): pp. 2261–69. <https://doi.org/10.1016/j.compstruc.2003.10.028>.
- [11] Spitas, V., G. Papadopoulos, Th. Costopoulos, and C. Spitas. Experimental Evaluation of Stress Intensity Factors in Spur Gear Teeth. In *Fracture of Nano and Engineering Materials and Structures*, edited by E. E. Gdoutos, 1239–40. Dordrecht: Springer Netherlands, 2006. [https://doi.org/10.1007/1-4020-4972-2\\_615](https://doi.org/10.1007/1-4020-4972-2_615).

- [12] Source, M., L. Reis, and M. Freitas. Failure Analysis of a Gear Wheel of a Marine Azimuth Thruster. *Engineering Failure Analysis* 18, fasc. 7 (October 2011): pp. 1884–88. <https://doi.org/10.1016/j.engfailanal.2011.07.009>.
- [13] Jelaska D., Podrug S., Gear tooth root fatigue behaviour. *Advanced Engineering*, 2007, vol. 2, pp.187-197
- [14] N. Sukumar, N. Moës, B. Moran and T. Belytschko, Extended finite element method for three-dimensional crack modelling, *International Journal for Numerical Methods in Engineering* Vol. 48(11), 2000 pp. 1549–1570.
- [15] Kramberger, J., M. Šraml, I. Potrč, and J. Flašker. Numerical Calculation of Bending Fatigue Life of Thin-Rim Spur Gears. *Engineering Fracture Mechanics* 71, fasc. 4–6 (March 2004): pp. 647–56. [https://doi.org/10.1016/S0013-7944\(03\)00024-9](https://doi.org/10.1016/S0013-7944(03)00024-9).
- [16] Santosh S. Patil, Saravanan Karuppanan and Ivana Atanasovska. Experimental Measurement of Strain and Stress State at the Contacting Helical Gear Pairs. *Measurement* 82 (March 2016): pp. 313–22. <https://doi.org/10.1016/j.measurement.2015.12.046>.
- [17] José A., Brandão, Jorge H.O. Seabra and Jorge Castro. Surface Initiated Tooth Flank Damage. *Wear* 268, fasc. 1–2 (January 2010): pp. 1–12. <https://doi.org/10.1016/j.wear.2009.06.020>.
- [18] Isaac J. Hong, Ahmet Kahraman and Neil Anderson. A Rotating Gear Test Methodology for Evaluation of High-Cycle Tooth Bending Fatigue Lives under Fully Reversed and Fully Released Loading Conditions. *International Journal of Fatigue* 133 (April 2020): 105432. <https://doi.org/10.1016/j.ijfatigue.2019.105432>.
- [19] S. Rajesh, P. Marimuthu, P. Dinesh Babu and R. Venkatraman. Contact Fatigue Life Estimation for Asymmetric Helical Gear Drives. *International Journal of Fatigue* 164 (November 2022): 107155. <https://doi.org/10.1016/j.ijfatigue.2022.107155>.

- [20] Vincent Argoud, Franck Morel, Etienne Pessard, Daniel Bellett, Simon Thibault and Stéphane Gourdin. Fatigue Behaviour of Gear Teeth Made of Case Hardened Steel: From Competing Mechanisms to Lifetime Variability. *Procedia Structural Integrity* 19 (2019): 719–28. <https://doi.org/10.1016/j.prostr.2019.12.078>.
- [21] Emil Weresa, Andrzej Seweryn, Jarosław Szusta and Zdzisław Rak. Fatigue Testing of Transmission Gear. *Eksploatacja i Niezawodność - Maintenance and Reliability* Vol.17, fasc. 2 (28 March 2015): pp. 207–14. <https://doi.org/10.17531/ein.2015.2.6>.
- [22] Gorla Carlo, Francesco Rosa, Edoardo Conrado and Horacio Albertini. Bending and Contact Fatigue Strength of Innovative Steels for Large Gears. *Proceedings of the Institution of Mechanical Engineers, Part C: Journal of Mechanical Engineering Science* 228, fasc. 14 (October 2014): 2469–82. <https://doi.org/10.1177/0954406213519614>.
- [23] Edward E. Osakue, Lucky Anetor. Contact fatigue design of helical gear by spur gear equivalency. *International Journal of Research in Engineering and Technology* 06, fasc. 02 (February 2017): pp. 30–44. <https://doi.org/10.15623/ijret.2017.0602006>.
- [24] Franco Concli, Lorenzo Fraccaroli and Lorenzo Maccioni. Gear Root Bending Strength: A New Multiaxial Approach to Translate the Results of Single Tooth Bending Fatigue Tests to Meshing Gears. *Metals* 11, fasc. 6 (25 May 2021): 863. <https://doi.org/10.3390/met11060863>.
- [25] Luca Bonaiti, Ahmed Bayoumi Mahmoud Bayoumi, Franco Concli, Francesco Rosa and Carlo Gorla. Gear Root Bending Strength: A Comparison Between Single Tooth Bending Fatigue Tests and Meshing Gears. *Journal of Mechanical Design* 143, fasc. 10 (March 2021): pp. 1-17. <https://doi.org/10.1115/1.4050560>.
- [26] You Lv, Bo Cui, Zhaolong Sun, Xinlei Xiao, Effects of discrete laser surface melting on the fatigue performance of 20CrMnTi steel gear, *Optics & Laser Technology*, Volume 171, 2024, 110359, <https://doi.org/10.1016/j.optlastec.2023.110359>.

- [27] You Lv, Liqun Lei, Lina Sun, Bo Cui, Improvement of the wear resistance of 20CrMnTi steel gear by discrete laser surface melting, *Optics & Laser Technology* Volume 165, October 2023, 109598, <https://doi.org/10.1016/j.optlastec.2023.109598>
- [28] Zhiyuan Wang, Kun Zhang, Lubing Shi, Dongfei Wang, Hechen Xing, Experimental and Numerical Investigations on Gear Root Crack Propagation Behavior and Fatigue Life, *J Fail. Anal. and Preven.* (2025) 25:445–457  
<https://doi.org/10.1007/s11668-025-02119-5>.
- [29] F. Curà, A. Mura, C. Rosso, Influence of high speed on crack propagation path in thin rim gears, *Fatigue Fract Engng Mater Struct*, 2017, 40, 120–129. DOI: 10.1111/ffe.12481.
- [30] Lewicki, D.G.; Ballarini, R. Effect of rim thickness on gear crack propagation path. *J. Mech. Des.* 1997, 119, 88–95.
- [31] Yunxia Chen, Yi Jin, Xihui Liang, Rui Kang, Propagation path and failure behavior analysis of cracked gears under different initial angles, *Mechanical Systems and Signal Processing* 110 (2018) 90–109.
- [32] Jay Govind Verma, Sachin Kumar, Pavan Kumar Kankar, Crack growth modeling in spur gear tooth and its effect on mesh stiffness using extended finite element method, *Engineering Failure Analysis* 94 (2018) 109–120.
- [33] W. J. Dixon and A. M. Mood, A., Method for Obtaining and Analyzing Sensitivity Data. *Journal of the American Statistical Association*, (1948) Vol. 43, No. 241, p. 109 – 126.
- [34] SAE Standard J1619 1997-01-01. Single tooth gear bending fatigue test.
- [35] Standard ISO 6336, Calculation of Load Capacity of Spur and Helical Gears, Part 1–6, International Standard Organization.